Journal of Electronic Research and Application, 2025, Volume 9, Issue 4
http://ojs.bbwpublisher.com/index.php/JERA
ISSN Online: 2208-3510
ISSN Print: 2208-3502

Prediction of the Ultraviolet Luminescence Potential of Bi_2SeO_5: First-Principles Insights

Yining Zhou[1,2], Jiamin Li[1,2], Yutong Feng[1,2], Yichen Bian[1,2], Longlinsen He[1,2], Chen-Min Dai[1,2]*

[1]Key Laboratory of Intelligent Optoelectronic Devices and Chips of Jiangsu Higher Education Institutions, School of Physical Science and Technology, Suzhou University of Science and Technology, Suzhou 215009, China
[2]Advanced Technology Research Institute of Taihu Photon Center, School of Physical Science and Technology, Suzhou University of Science and Technology, Suzhou 215009, China

**Corresponding author: : daichenmin@usts.edu.cn*

Abstract: As a new layered semiconductor material, Bi_2SeO_5 has shown potential in the field of ultraviolet electronic devices in recent years because of its unique crystal structure and wide band gap. In this paper, the crystal structure, electronic structure, and thermodynamic stability of Bi_2SeO_5 are studied based on first-principles calculations. The ultraviolet luminescence property of Bi_{Se} defect is predicated from defect property, which provides theoretical basis for experimental design of high-performance Bi_2SeO_5 photoelectric devices.

Keywords: First-principles calculation; Bi_2SeO_5; Ultraviolet luminescence property

1. Introduction

Traditional ultraviolet (UV) light sources are difficult to be portable, integrated, and automated due to their large size and power consumption. Compared with traditional UV light sources, nitride-based UV light sources have the advantages such as environmental friendliness, compact portability, ease of integration, tunable wavelengths, and long carrier lifetime. Therefore, nitride-based materials have great potential in UV luminescence applications. Although nitride UV sources have been widely used in secure communication, UV curing, optical medicine, and other fields, the low efficiency of luminescence is still an urgent problem to be solved, mainly due to the difficulty of p-type doping and the low carrier mobility. The preparation of high-quality materials and the realization of p-type doping are closely related to the defect properties of nitride. Effectively passivating defects to produce high-quality nitride materials persists as a significant technical hurdle.

Semiconductors ($CsPbI_3$, Sb_2Se_3, Sb_2S_3, GeSe, etc.) containing lone-pair electrons are usually defect-tolerant, that is, the defects with low formation energy have shallow defect levels, while the deep level defects have high formation energy [1–6]. Using Bi_2SeO_5 as a gate dielectric layer, a high-performance field effect transistor can be fabricated with low subthreshold swing, high current on/off ratios, and high mobility, which proves the high quality of the dielectric layer and few interface defects [7].

However, little research has been done on Bi_2SeO_5. In 2001, Rademacher *et al.* successfully prepared Bi_2SeO_5. Unfortunately, they only described the crystal structure and did not study the material properties [8]. Subsequently, in 2004, Dityatyev *et al.* used neutron powder diffraction data to determine the crystal structure of Bi_2SeO_5, and studied its evolution with temperature [9]. In recent years, theoretical studies on Bi_2SeO_5 have gradually increased [10–15]. In this paper, the crystal structure, electronic structure, and thermodynamic stability of Bi_2SeO_5 are studied based on first-principles calculation. The ultraviolet luminescence of Bi_{Se} defect is predicted from the defect property, which provides a theoretical basis for experimental design of Bi_2SeO_5 high-performance photoelectric devices.

2. Crystal and electronic structure

The primitive cell of Bi_2SeO_5 contains 32 atoms, including 8 Bi atoms, 4 Se atoms, and 20 O atoms. Based on the symmetry of the crystal space group and the chemical environment of atomic bonding, there are three nonequivalent positions of Bi, six nonequivalent positions of O, and one nonequivalent position of Se in Bi_2SeO_5.

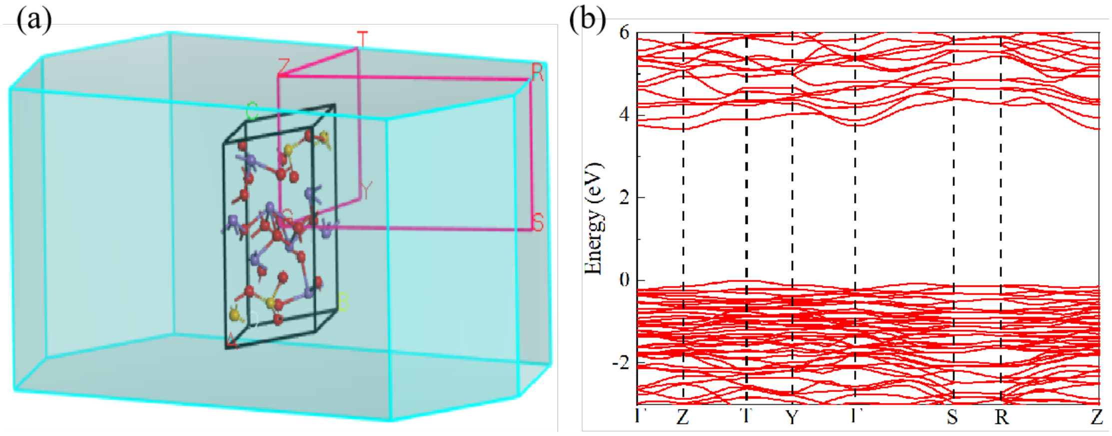

Figure 1. (a) The Brillouin zone and (b) band gap of Bi_2SeO_5.

In order to calculate the band gap of Bi_2SeO_5, we construct the Brillouin zone of Bi_2SeO_5 through its crystal lattice characterization system. Based on the symmetry of the Brillouin zone, we then determine the high-symmetry paths and plan the required reciprocal space k-points for calculations. As shown in **Figure 1(a)**, the black line represents the crystal structure of Bi_2SeO_5 with ABM space group, and its optimized lattice constants $a = b = 8.77$ Å, $c = 11.62$ Å. The reciprocal space basis vectors are derived through the periodicity of the Bravais lattice and the Fourier transform of real-space basis vectors. The boundaries of the Brillouin zone are formed by the perpendicular bisecting planes of reciprocal lattice vectors, with the gray polygonal region enclosed by the blue lines representing the first Brillouin zone of Bi_2SeO_5 in reciprocal space. Based on the symmetry of the Brillouin zone, the pink high-symmetry paths are extracted, and the high symmetry k-points (Γ (0,0,0), Z (0,0,0.5), T (-0.5, 0.5, 0.5), Y (-0.5, 0.5, 0), S (0, 0.5, 0) and R (0, 0.5, 0) that can completely reflect the topological characteristics of the energy band are selected. Connect successively adjacent high-symmetry points in the Brillouin zone to form a Γ→Z→T→Y→Γ→S→R→Z closed path. On the high-symmetry path, symmetric points are sampled at equal intervals using the uniform interpolation method. The 20 k-points are selected along the Γ-Z path, 28 k-points along the Z-T path, 20 k-points along the T-Y path, 28 k-points along the Y-Γ path, 44 k-points along the Γ-S path, 20 k-points along the S-R path, and 44 k-points along the R-Z path. This results in a total of 204 k-points sampled across all high-symmetry paths. This k-point density can accurately capture band extremes while avoiding computational resource wastage caused by an excessive number of k-points.

Based on the first-principles calculation, we can plot the electronic band structure. First, the structure optimization of Bi_2SeO_5 is performed to ensure both the lattice constants and the atoms' positions in equilibrium and stable state. In order to overcome the underestimation of the band gap by GGA, we employ the HSE hybrid function to correct the energy levels calculated by GGA. By mixing 18% Hartree-Fock exact exchange energy with 82% PBE exchange correlation energy, the accuracy of band gap calculation is effectively improved. The first principle calculations show that Bi_2SeO_5 is an indirect bandgap semiconductor, the CBM is at Z point, the VBM is at T point, and the value of the band gap is 3.7 eV. The corresponding optical absorption edge of the wide band gap is 335 nm, indicating that Bi_2SeO_5 can meet the UV luminescence requirements of shorter wavelengths. This approach provides theoretical guidance for designing UV Bi_2SeO_5 light-emitting diodes (LEDs).

3. Thermodynamic stability

In order to synthesize single-phase Bi_2SeO_5, the chemical formulas of the constituent elements (Bi, Se, and O) must satisfy a series of thermodynamic conditions. First, the chemical potential should be satisfied.

$$2\mu_{Bi} + 5\mu_O + \mu_{Se} = \Delta H_f(\mathrm{Bi_2SeO_5})$$

Here, μ_i is the chemical potential of element *i* (Bi, Se, and O), $\Delta H_f(\mathrm{Bi_2SeO_5})$ represents the formation enthalpy of Bi_2SeO_5. Second, to avoid the decomposition of Bi_2SeO_5 into any Bi, O, or Se elemental, binary, and ternary compounds. For example, Bi, O_2, Se, Bi_2O_3, Bi_2Se_3, BiO_2, $BiSe_2$, Se_2O_5, SeO_2, Bi_2O_2Se, $Bi_2Se_3O_{10}$ and $Bi_2Se_3O_9$ should also meet multiple inequality conditions, taking Bi_2O_3 as an example:

$$2\mu_{Bi} + 3\mu_O < \Delta H_f(\mathrm{Bi_2O_3})$$

Based on the above restrictions, we can determine the range of elemental chemical potentials that need to be satisfied to form pure Bi_2SeO_5. As the chemical potential of O becomes poorer, the main competing phases of Bi_2SeO_5 are Bi_2O_3. As the chemical potential of Se becomes richer, Bi_2Se_3 and $Bi_2Se_3O_9$ are the main competing phases. Therefore, the preparation of high-quality single crystal Bi_2SeO_5 requires stricter control of μ_{Se}.

4. Defect-induced photoluminescence

The photoluminescence mechanism induced by defects in semiconductors involves the process where charge carriers are photoexcited to an excited state and subsequently return to the ground state through radiation recombination, releasing photons. This paper adopts configuration coordinate diagrams combined with a one-dimensional vibrational approximation to investigate the UV luminescence property of Bi_2SeO_5. For the radiation transition, the configuration coordinate diagram of Bi_{Se1} defect is drawn, which shows the excitation and emission process of the charge carrier.

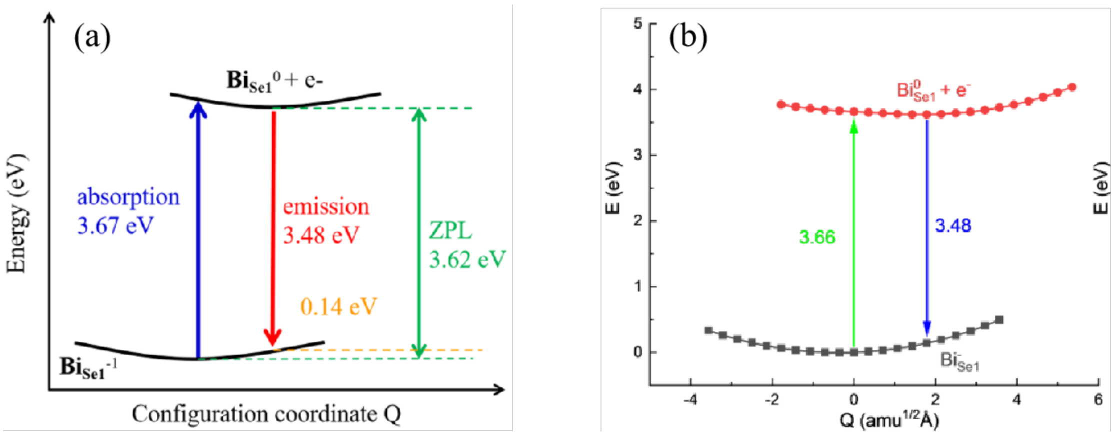

Figure 2. (a) Configuration coordinate diagram of the photoluminescence in BiSe defect and (b) a harmonic vibrational potential energy surface of BiSe defect luminescence process.

For the $\mathrm{Bi_{Se}}$ defect under the condition of p-type conduction, it exhibits a tendency to accept electrons, which is an acceptor, resulting in a relatively high concentration of $\mathrm{Bi_{Se}^{-}}$. The $\mathrm{Bi_{Se}^{-}}$ defect state is the ground state, the photoexcitation process causes the valence state of $\mathrm{Bi_{Se}}$ defect to transition from the ground state $\mathrm{Bi_{Se}^{-}}$ to the excited state $\mathrm{Bi_{Se}^{0}}$ (the electron on the $\mathrm{Bi_{Se}^{-}}$ defect level is excited to the CBM, generating an electron at CBM). The electron in the $\mathrm{Bi_{Se}^{0}}$ excited state is relaxed, then transitions back to the $\mathrm{Bi_{Se}^{-}}$ ground state to generate a photon. For the electron trapping process of the defect, the energy of the zero phonon line is the difference value between the band gap and the transition level. As shown in **Figure 2(a)**, the relaxation energy between the -1 and neutral valence states of $\mathrm{Bi_{Se}}$ is very small (only 0.14 eV). When excited by the light with energy of 3.67 eV, $\mathrm{Bi_{Se}}$ can emit UV light with energy of 3.48 eV, indicating a potential UV light source. The transition between the ground and excited states of $\mathrm{Bi_{Se}}$ occurs on a harmonic vibrational potential energy surface, as depicted in **Figure 2(b)**. The minimal shift in the normal coordinate ΔQ signifies an extremely small structural distortion induced by photoexciting in $\mathrm{Bi_{Se}}$ defect, further supporting its viability as a potential UV light source.

5. Conclusion

As a new layered semiconductor material, $\mathrm{Bi_2SeO_5}$ has shown great potential in the field of UV optoelectronic devices due to its unique crystal structure and wide band-gap. In this paper, we systematically analyze the physical basis and technical advantages of the ultraviolet luminescence performance of $\mathrm{Bi_2SeO_5}$ from its crystal structure, thermodynamic stability, electronic structure, and luminescence mechanism of $\mathrm{Bi_{Se}}$ defect. The first-principles theoretical calculation provides a theoretical basis for the experimental design of high-performance $\mathrm{Bi_2SeO_5}$ optoelectronic devices.

Funding

This work was supported by the National Natural Science Foundation of China under Grant No. 12404093 and the China Postdoctoral Science Foundation under Grant No. 2021M702915.

Disclosure statement

The authors declare no conflict of interest.

References

[1] Liu SC, et al., 2021, An Antibonding Valence Band Maximum Enables Defect-Tolerant and Stable GeSe Photovoltaics. Nature Communications, 12: 670.

[2] Huang M, et al., 2021, More Se Vacancies in Sb_2Se_3 under Se-Rich Conditions: An Abnormal Behavior Induced by Defect-Correlation in Compensated Compound Semiconductors. Small, 17: 2102429.

[3] Cai Z, et al., 2020, Intrinsic Defect Limit to the Electrical Conductivity and a Two-Step P-Type Doping Strategy for Overcoming the Efficiency Bottleneck of Sb_2S_3-Based Solar Cells. Solar RRL, 4: 1900503.

[4] Cai Z, et al., 2020, Extrinsic Dopants in Quasi-One-Dimensional Photovoltaic Semiconductor Sb_2S_3: A First-Principles Study. The Journal of Applied Physics, 127.

[5] Xue H, et al., 2023, Compound Defects in Halide Perovskites: A First-Principles Study of $CsPbI_3$. The Journal of Physical Chemistry C, 127: 1189.

[6] Huang M, et al., 2019, Complicated and Unconventional Defect Properties of the Quasi-One-Dimensional Photovoltaic Semiconductor Sb_2Se_3. ACS Applied Materials & Interfaces, 11: 15564.

[7] Li T, et al., 2020, A Native Oxide High-Kgate Dielectric for Two-Dimensional Electronics. Nature Electronics, 3: 473.

[8] Rademacher O, et al., 2001, Crystal Structure of Dibismuth Selenium Pentoxide Bi_2SeO_5. Zeitschrift fur Kristallographie - New Crystal Structures, 216: 29.

[9] Dityatyev OA, et al., 2004, Phase Equilibria in the Bi_2TeO_5-Bi_2SeO_5 System and a High Temperature Neutron Powder Diffraction Study of Bi_2SeO_5. Solid State Sciences, 6: 915.

[10] Dong X, et al., 2024, Exploring the High Dielectric Performance of Bi_2SeO_5: From Bulk to Bilayer and Monolayer. Science China Materials, 67: 906.

[11] Ling D, et al., 2023, Oxygen Vacancy-Enriched Bi_2SeO_5 Nanosheets with Dual Mechanism for Ammonium-Ion Batteries. ACS Nano, 17: 25222.

[12] Park H, et al., 2024, Direct Growth of Bi_2SeO_5 Thin Films for High-k Dielectrics via Atomic Layer Deposition. ACS Nano, 18: 22071,

[13] Liu H, et al., 2025, First-Principles Insights into Bi_2XO_5 (X = Se, Te) Monolayers as High-k Gate Dielectrics for 2D Electronics, Applied Physics Letters, 126: 072901.

[14] Liu C, et al., 2022, Self-Assembled Bi_2SeO_5/rGO/MIL-88A Z-Scheme Heterojunction Boosting Carrier Separation for Simultaneous Removal of Cr (VI) and Chloramphenicol. Chemical Engineering Journal, 431: 133289.

[15] Liang S, et al., 2019, Phase Transformation Synthesis of a New Bi_2SeO_5 Flower-Like Microsphere for Efficiently Photocatalytic Degradation of Organic Pollutants, Catalysis Today, 327: 357.